Estimating forage quantity and quality under different stress and senescent biomass conditions via spectral reflectance

Martín Durante[a], Martín Oesterheld[a], Gervasio Piñeiro[a] & María
Mercedes Vassallo[a]

[a] Laboratorio de Análisis Regional y Teledetección, IFEVA, Faculty
of Agronomy, University of Buenos Aires, Conicet, C1417DSE
Buenos Aires, Argentina
Published online: 27 Mar 2014.

PLEASE SCROLL DOWN FOR ARTICLE

Taylor & Francis
Taylor & Francis Group

Estimating forage quantity and quality under different stress and senescent biomass conditions via spectral reflectance

Martín Durante*, Martín Oesterheld, Gervasio Piñeiro, and María Mercedes Vassallo

Laboratorio de Análisis Regional y Teledetección, IFEVA, Faculty of Agronomy, University of Buenos Aires, Conicet, C1417DSE Buenos Aires, Argentina

Assessing forage quantity and quality through remote sensing can facilitate grassland and pasture management. However, the high spatial and temporal variability of canopy conditions may limit the predictive accuracy of models based on reflectance measurements. The objective of this work was to develop this type of models, and to challenge their capacity to predict plant properties under a wide range of environmental conditions. We manipulated *Paspalum dilatatum* canopies through different stress treatments (flooding, drought, nutrient availability, and control) and by artificially varying the amount of senescent biomass. We measured canopy reflectance and constructed simple models, based on either normalized vegetation indices or a few selected wavebands, to estimate biomass and two variables related to forage quality: proportion of photosynthetic vegetation and biomass C:N ratio. General models satisfactorily predicted plant properties for the whole set of environmental conditions, but failed under specific conditions such as drought (for estimates of plant biomass), fertilization (for estimates of C:N ratio), and different levels of senescent tillers (for estimates of the proportion of photosynthetic vegetation). Where general models failed, specific models, based on different bands, achieved satisfactory accuracy. The general models performed better when based on a few selected bands than when based on two-band vegetation indices, having better accuracy (higher R^2) and parsimony (lower BIC). However specific models performed similarly for both approaches (similar R^2 and BIC). These results indicate that these plant properties can be predicted from reflectance information under a broad range of conditions, but not for some particular conditions, where ancillary data or more complex models are probably needed to increase predictive accuracy.

1. Introduction

Farmers need near real-time information of forage quality and quantity at the paddock scale to properly manage forage resources (Diaz-Solis et al. 2006; Grigera, Oesterheld, and Pacin 2007; Phillips et al. 2009). A cattle management system in which forage allowance (kg forage/kg body weight) is regulated on a seasonal basis can improve animal performance and forage condition (Soca and Orcasberro 1992; Jochims et al. 2013). It is easy to find the divisor of this ratio, the stocking rate, but it is difficult to determine the dividend, forage biomass, due to its variable nature in both time and space. In addition, forage biomass may widely vary in its quality (i.e. in its capacity to be consumed, assimilated, and transformed into animal products (Huston and Pinchak 1991)). Estimations of forage quantity and quality based on remote sensing at moderate spatial resolution could capture this variation and serve as a tool for decision-making (Phillips et al. 2009).

---

*Corresponding author. Email: durante@agro.uba.ar

However, the predictive capacity of models assessing plant properties through canopy reflectance is often limited to a set of conditions which limits its utilization for decision-making. Canopy reflectance measured by remote sensors integrates physical and biological process occurring on the ground (Roberts et al. 2004). Due to the convergence among plant traits (Grime 1977), many plant properties may be confidently estimated by a few absorption features. For example, the normalized difference vegetation index (Tucker 1977) can estimate leaf area index (Thenkabail, Smith, and De Pauw 2000), chlorophyll concentration (Reddy et al. 2001), leaf biomass (Freitas, Mello, and Cruz 2005), nitrogen deficiency (Peñuelas et al. 1994), and vegetation cover (Reddy et al. 2001), among others. However, the ability of canopy reflectance to estimate plant properties is often context dependent, which may hinder the ability to estimate a given plant property under other environmental conditions than those for which relations between reflectance and the plant property were tested (Ollinger 2011). It is then necessary to identify specific relations between plant and spectral properties to develop reliable models, capable of being used under a wide range of conditions.

Since biomass and forage quality of grasslands and pastures are highly variable in both space and time, a single model may not be applicable to a wide range of field conditions (Jackson and Huete 1991; Kokaly and Clark 1999). Variation in space is due to abiotic factors such as soil characteristics, topography, aspect, water and nutrient availability, and the interaction with grazer preferences, conditioned by landscape characteristics and human intervention (fences, distance to water). Variation in time is mainly caused by grazing events, phenological changes, and weather conditions. Biomass and forage quality and their variation can be studied using manipulative experiments, field studies, and simulation models. Typically, field studies can explore a narrower range of canopy conditions than manipulative experiments or simulation models. At the landscape level there is some empirical evidence that forage quality and quantity estimations are unaffected by water stress, seasonal variance, and grazing (Beeri et al. 2007; Phillips, Beeri, and Liebig 2006; Cho and Skidmore 2009). In addition, simulation models allow the identification of bands related to forage properties and insensitive to changes in solar zenith angle (Cho, Skidmore, and Atzberger 2008). However, we found no manipulative experiments that explore a wide range of canopy and environmental conditions. It is important to identify those environmental conditions that affect the relationship between spectral reflectance and plant properties, to determine the extent and limitations of model estimates of forage quantity and quality based on reflectance.

The plant–light interactions that allow one to infer the quantity and quality of plant biomass are scale dependent, with an increasing complexity from individual leaf to canopy (Ollinger 2011). At the leaf scale, spectra for all types of vegetation share some basic features. Green leaves strongly absorb in the visible region (400–700 nm), due to pigment composition, and reflect in the near-infrared region (700–1300 nm), due to photon scattering in the mesophyll. Another common feature is the strong water absorption around 1450 and 1950 nm (Asner 1998), which may obscure other minor absorption features related with the concentration of organic compounds (i.e. cellulose, lignin, protein, waxes, oil, sugar, starch) that partially overlap with the region of water absorption (SWIR I 1300–1900 nm and SWIR II 1900–2500 nm; Curran 1989; Elvidge 1990). Finally, individual green and senescent leaves differentially absorb radiation in the 400–800 nm region (Asner 1998). At the canopy scale, the amount and distribution of senescent and green leaf area and soil cover are the dominant controls of reflectance (Asner 1998). These basic features are useful for inferring different canopy properties. For example, bands in the green region (540–560 nm) and in the red edge (the shift between

visible and near-infrared), where chlorophyll absorption is low, are useful in the detection of chlorophyll concentration (Filella and Peñuelas 1994; Hatfield et al. 2008), while a minor absorption feature related to cellulose (a C–H bond stretch overtone at 1722 nm) allows the estimation of biomass (Wang et al. 2011).

Two commonly used methods to assess plant properties through remote sensing are the identification of two-band vegetation indices and band selection procedures based on multivariate analysis. The normalized vegetation index, the ratio between the difference and the sum of the reflectance of two bands, was used to estimate biomass quantity (Gamon et al. 1995; Thenkabail, Smith, and De Pauw 2000) and quality (Phillips, Beeri, and Liebig 2006). Partial least squares analysis is a multivariate technique that facilitates processing of the high dimensionality and collinearity of hyperspectral data (Carrascal, Galván, and Gordo 2009). The combination of full-spectrum, partial least squares models and band selection techniques eliminates redundant information and facilitates interpretation of the selected bands from a biophysical approach (Clevers et al. 2007; Darvishzadeh et al. 2008; Kawamura et al. 2008, 2010).

The objective of this work was to develop models to estimate forage quantity and quality from reflectance measurements, and challenge their predictive capacity under a wide range of environmental conditions. We manipulated canopies of *Paspalum dilatatum*, a native perennial grass from the Pampean region in Argentina, to obtain a wide range of variation in forage quantity and quality. Canopy variations were generated by different stress treatments (flooding, drought, nutrient availability, and control) and by artificially varying the amount of senescent biomass. We constructed simple models, based on either normalized vegetation indices or a few selected wavebands, to estimate biomass and two variables related with quality: proportion of photosynthetic vegetation and C:N ratio. We evaluated: (1) the predictive accuracy of general models constructed for the whole dataset to include a wide range of environmental conditions; (2) the systematic error associated with particular conditions given by treatments; and (3) the need for generation of specific models under particular conditions to improve model accuracy.

2. Material and methods

2.1. Experimental set-up

We carried out an experiment in a controlled-condition glasshouse at the Faculty of Agronomy, University of Buenos Aires (lat. 34° 35′ S, long. 58° 28′ W). The experiment produced a wide variation in the quantity and quality of plant biomass and the proportion of senescent biomass. *Paspalum dilatatum* specimens were collected from natural grasslands of the Flooding Pampa region, where this species is a dominant and valuable forage. Plants were propagated vegetatively to yield 160 individuals for the experiment. Each individual plant was placed in a pot filled with 50% natural grassland soil and 50% sand to improve soil permeability (a total of 2413 cm^3 of substrate). The plants were randomly assigned to one of four environmental treatments: flooding, fertilization, drought, or control (40 plants per treatment). Flooded plants were watered daily to maintain 3 cm of water above the soil surface. Fertilized plants received an initial dose of 1.2 g of triple superphosphate and 1 g of urea. Pots of fertilized, control, and drought treatments were weighed and watered daily. Based on pot weight and substrate texture, the two former treatments received water to attain field capacity, while the drought treatment was watered to reach 50% field capacity. In order to maximize the variation in canopy conditions,

within each treatment, half of the plants were left intact and half were initially pruned to a height of 6 cm. The experiment started on 17 November and ended on 17 December 2008.

Measurements of spectral and plant properties were conducted on four dates (17 November and 1, 10, and 17 December). In order to relate biomass and C:N ratio to spectral properties on each date, the spectral reflectances of 10 individual pots of each treatment (5 clipped and 5 unclipped) were measured (4 dates × 4 treatments × 10 replicates, $n = 160$). Coverage of each individual plant was around 500 cm^2 (37% of the measured area – see below). In order to relate the mass proportion of photosynthetic vegetation to spectral properties on each date, the spectral radiances of three replicates of four groups of three control pots combining pruned and unpruned pots (0, 1, 2, and 3 clipped pots per group) were measured under three levels of senescent biomass. The three levels of senescent biomass were generated by manually adding to each pot 0, 1, or 3 senescent tillers of known mass mimicking their natural position (4 dates × 3 levels of extra senescent biomass × 4 groups of pots × 3 replicates, $n = 144$). After spectral measurement, all pots were harvested in preparation for measurement of a suit of plant properties (see Section 2.3).

2.2. Spectral reflectance

Spectral radiance was measured using a portable spectroradiometer (Field-Spec Pro FR; Analytical Spectral Devices [ASD], Boulder, CO, USA) with a 25° field of view and a spectral sampling of 1.4 nm in the 350–1000 nm range and 2 nm in the 1000–2500 nm range. Spectral resolution is 3 nm in the 350–1000 nm range and 10 nm in the 1000–2500 nm range, calculated to 1 nm resolution wavelength for output data using a cubic spline interpolation function in ASD software (RS2 for Windows). A spectralon reference panel (Labsphere Inc.) was used as white reference to calculate reflectance.

In order to control for atmospheric, illumination, and background conditions, measurements were made within a box (150 cm height × 50 cm width) whose interior was painted black (matt black No 63476, Krylon, Sherwin Williams). The sensor was inside the box, 95 cm above the base of the canopy, producing a viewing area of diameter 41.5 cm. Around and above the sensor were placed four 150 W tungsten lamps (Philips Spotline R95, Buenos Aires, Argentina). A black-painted tray covered the pot soil and the space between pots, with the plant canopy emerging above the tray through a hole. In this way, only the canopy was measured while the background was kept constant. White standards with the reference panel were taken inside the black box every 10 minutes.

2.3. Plant properties

On each date, all measured plants were harvested. Above-ground plant biomass was separated into green blades, senescent blades, green sheaths, senescent sheaths, and inflorescences (not separated into green and senescent), and each component was dried and weighed. A sub-sample of each plant component was ground using a mortar grinder and then analysed for total C and N by dry combustion using a LECO CN analyser (LECO, Corp., St. Joseph, MI). Green and senescent materials were analysed separately. Total biomass was computed as the sum of all plant components. The mass proportion of photosynthetic vegetation was estimated as the ratio between green and total (green + senescent) blades and sheaths, considering both natural and added biomass. C:N ratio was calculated as the ratio between the mass concentration of C and N. As expected, the three plant properties varied widely across dates and treatments (Table 1).

Table 1. Descriptive statistics for plant biomass (B), C:N ratio, and the proportion of photosynthetic vegetation (PV) for the whole data set (All) and for each treatment separately.

Plant property	Treatment	Statistical descriptor				
		Minimum	Mean	Maximum	SD	CV
B (gm^{-2})	All	34	99	262	47	0.47
	Control	38	88	172	31	0.35
	Flooded	39	100	180	34	0.34
	Nitrogen	38	141	262	60	0.43
	Drought	34	68	105	19	0.28
C:N ratio	All	18	51	98	18	0.35
	Control	39	58	83	12	0.2
	Flooded	38	53	71	9	0.17
	Nitrogen	18	29	45	9	0.32
	Drought	45	66	98	17	0.26
PV	All	0.36	0.61	0.91	0.15	0.24
	0	0.66	0.77	0.91	0.06	0.08
	1	0.52	0.62	0.75	0.06	0.09
	3	0.36	0.44	0.51	0.04	0.09

Note: SD, standard deviation; CV, coefficient of variation. The number of observations was 160 for B and C:N, and 144 for PV.

2.4. Spectral data analysis

Prior to the analysis, spectral data were restricted to the 400–2400 nm range because of the high spectral noise outside that range. Additionally, the remaining bands were averaged at 5 nm wavelength intervals in order to reduce the size of the data set (400 bands). Then, we used empirical regression analysis to explain the variation in the three plant properties based on these processed spectra. When working with hyperspectral data, bands often exceed the number of observations, are highly correlated, and contain redundant information. As a consequence, overfitting and collinearity may limit the calculation and interpretation of the linear regression equations (Carrascal, Galván, and Gordo 2009; Kawamura et al. 2008). Additionally, as we were not only interested in getting a good predictive model, but also in assessing whether the bands included in the models were related to known biophysical properties, we tried to keep as few bands as possible. Thus, we estimated plant properties through linear regression models based on either two-band vegetation indices (VIs) or small sets of reflectance bands obtained by combining partial least squares models with waveband selection (multiband). For both approaches, we first selected one from many potential vegetation indices or sets of bands, and then evaluated the predictive accuracy of models developed with the selected indices or bands by a bootstrap procedure. Details on band selection and predictive accuracy testing are given below.

2.4.1. Band selection

For both approaches (VI and multiband), we selected the combination of wavebands with the minimum predictive error. Predictive error was assessed by the root mean squared difference (RMSD) from leave-one-out cross-validation:

$$\text{RMSD} = \sqrt{\frac{\sum_{i=1}^{n}(\hat{y}_i^c - y_i^c)^2}{n}}, \tag{1}$$

where $\hat{y}$ and y are the cross-validated predicted and measured values for the variables of interest, respectively, and n is the number of observations.

For models based on vegetation indices, the RMSD of all combinations of two out of 400 bands was compared (similarly to Mutanga and Skidmore 2004). For the multiband models, to better deal with the random component of the data, the selection procedure was more complex and consisted of three steps. The first step was a partial least squares model with stepwise waveband selection (similar to Kawamura et al. 2008) repeated 500 times for data sets randomly re-sampled with replacement. The partial least squares equation was as follows:

$$Y = \beta \mathbf{X} + \varepsilon, \tag{2}$$

where Y is a vector of the plant property observations, $\mathbf{X}$ is a matrix of reflectance values per spectral band, β is the matrix of weighted coefficients and ε is the error vector. A large absolute weighted value indicates an important $\mathbf{X}$ variable and thus, an informative band. The β matrix is calculated from the partial least square loadings of the model with the optimum number of latent variables. The minimum RMSD from leave-one-out cross-validation was used to select the optimum number of latent variables to be included in the regression models. Waveband selection was carried out stepwise, from the model with 400 bands to that with one band, by removing the band with the lowest β coefficient in each step (for more details see Kawamura et al. 2008). Because the re-sampling procedure has a random component, the band importance ranking (order of elimination) changed between iterations. We considered important those bands that appeared more often than expected by chance ($p < 0.01$) within the five final wavebands. Since the number of bands selected with this procedure was high (between 30 and 50), we performed a second selection step by eliminating bands that were correlated. The second step consisted of a hierarchical clustering based on Euclidean distance. We arranged correlated bands into six to eight groups and then calculated all the possible multiple linear regression models using one band from each group. The selected bands in this step were those included in the model with the lower RMSD. The third step for selecting wavebands consisted of using the Bayesian information criterion (BIC, Schwarz 1978) to select the best multiple regression model with those bands selected in step 2. The BIC is a criterion for model selection that penalizes models by their number of parameters to reduce over-fitting. The penalty value is higher in the BIC than in the Akaike criterion. The final number of bands in multiband models ranged between 4 and 7.

To test our band selection procedure, we compared the predictive accuracy between multiband models and the full spectrum partial least squared models (the initial models before band selection). RMSD did not differ between models, indicating that the band selection procedure gained simplicity at no significant cost to prediction ability.

2.4.2. Model predictive ability evaluation

A bootstrap procedure (similar to Mutanga, Skidmore, and Prins 2004) was applied to test the predictive accuracy and bias of the two approaches (VI and multiband). First, the full dataset, including data from all treatments, was divided into calibration and evaluation subsets ($n = 1000$ iterations). In order to evaluate the predictive accuracy of general models for a wide range of environmental conditions, we randomly extracted 70% of the data for calibration and 30% for evaluation from the whole data set. In order to evaluate the predictive accuracy of specific models for particular treatments, for validation we used

only a random subset (30%) of data from one treatment at a time. For each iteration, a regression model from the calibration subset was used to predict the plant properties in the evaluation subset, and some descriptors of the predictive accuracy of models were recorded and finally averaged. The descriptors of predictive accuracy calculated were: the coefficient of determination (R^2), the root mean squared difference (RMSD), and the relative error (RE), which provide a measure of the goodness-of-fit; and Theil's partial inequality coefficients and the slope and intercept of the fitted regression line between observed and predicted values, which provide a measure of the randomness of the error. Theil's partial inequality coefficients (Smith and Rose 1995) distinguish between different sources of predictive error: a proportion associated with mean differences between observed and predicted values (U_{bias}), a proportion associated with the slope (β) of the fitted model and the 1:1 line ($U\beta = 1$), and a proportion associated with the unexplained variance (U_e). The descriptors were calculated as follows:

$$U_{bias} = \frac{n(OBS - PRE)^2}{\sum_n (obs_i - pre_i)^2}, \tag{3}$$

$$U_{\beta=1} = \frac{(\beta - 1)^2 \sum_n (pre_i - PRE_i)^2}{\sum_n (obs_i - pre_i)^2}, \tag{4}$$

$$U_e = \frac{\sum_n (est_i - obs_i)^2}{\sum_n (obs_i - pre_i)^2}, \tag{5}$$

where 'obs' and 'pre' are the observed and predicted values, respectively; OBS and PRE are the means of the observed and predicted values, respectively; 'est' are the values estimated from the fitted regression model; and n is the number of observations in the validation dataset. Second, for those treatments in which general models had a significant non-random prediction error (i.e. the slope or the intercept of the fitted regression line between observed and predicted values differing from 1 and 0, respectively), two kinds of specific model using only the specific treatment dataset (70% calibration and 30% evaluation) were developed and tested: (1) models based on the same bands as the general models (re-parameterized) and (2) models with new band selection (based on new bands).

To evaluate the performance of VI against multiband models relative to the number of model parameters, we also used BIC (Schwarz 1978). BIC balances goodness-of-fit and model complexity (an undesired source of variance) in a single metric.

All data handling and calculations were performed with R software (R Development Core Team 2011), and PLS regression was analysed using the 'pls' package in R (Bjørn-Helge, Wehrens, and Liland 2011).

3. Results

General models based on canopy reflectance of a few bands closely captured variations in plant biomass, C:N ratio, and proportion of senescent biomass across a wide range of environmental conditions (Table 2, Figure 1). However, a significant reduction in model accuracy was observed under some specific environmental conditions. General multiband models, which were based on four to seven bands, presented higher fit and lower predictive error than general VI models, which were based on only two wavebands.

Table 2. Coefficient of determination (R^2), root mean square deviation (RMSD), relative error (RE), and Theil's partial inequality coefficients (U_e, U_{bias}, and $U\beta$) for observed *versus* cross-validated predicted values of plant biomass (B), C:N ratio, and the proportion of photosynthetic vegetation (PV) for multiband models and vegetation index (VI) models. Each value is the average (or standard deviation in brackets) of 1000 cross-validations that predicted 30% of the observations of each treatment on the basis of models generated from all other observations. The number of observations was 160 for B and C:N, and 144 for PV.

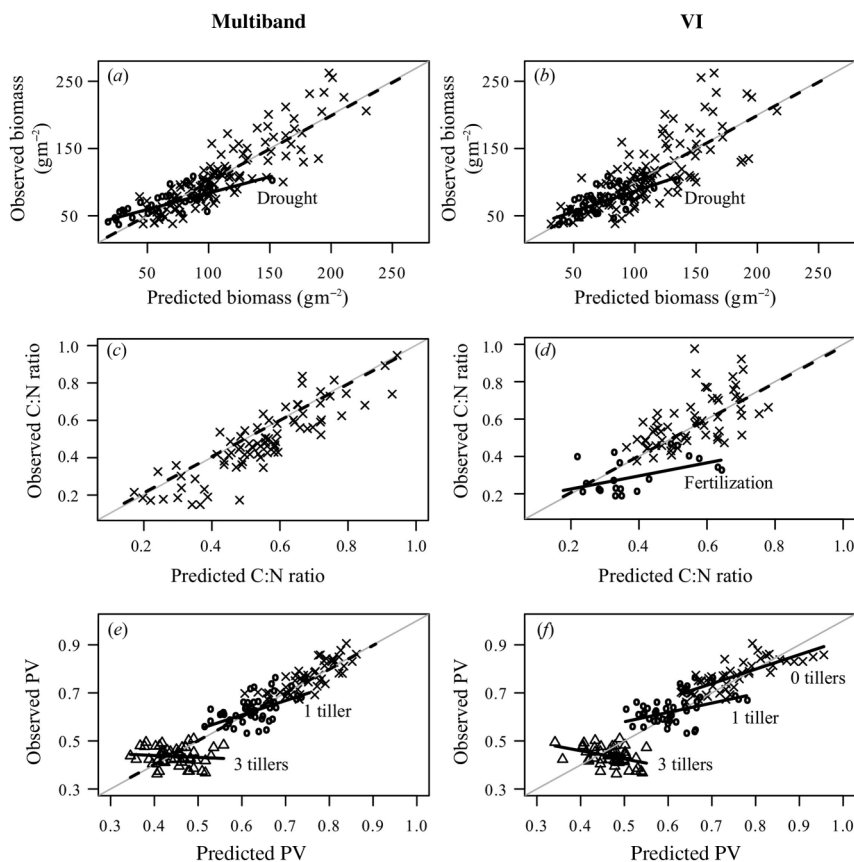|	Plant property	R^2		RMSD		RE		U_e		U_{bias}		$U\beta$	
Multiband	B (gm^{-2})	0.78	(0.05)	22.6	(2.2)	0.20	(0.02)	0.92	(0.09)	0.03	(0.04)	0.05	(0.07)
	C:N	0.78	(0.07)	8.77	(1.1)	0.17	(0.04)	0.87	(0.10)	0.06	(0.07)	0.07	(0.08)
	PV	0.87	(0.02)	0.05	(0.01)	0.08	(0.01)	0.94	(0.06)	0.03	(0.05)	0.03	(0.04)
VI	B (gm^{-2})	0.65	(0.06)	28.4	(3.1)	0.22	(0.03)	0.93	(0.07)	0.03	(0.04)	0.04	(0.05)
	C:N	0.54	(0.12)	12.5	(1.8)	0.23	(0.04)	0.89	(0.10)	0.05	(0.07)	0.06	(0.07)
	PV	0.81	(0.03)	0.07	(0.01)	0.10	(0.01)	0.93	(0.06)	0.03	(0.04)	0.04	(0.05)

Figure 1. Relationship between observed and predicted plant biomass, C:N ratio, and the proportion of photosynthetic vegetation (PV) for multiband (*a*, *c*, and *e* plots) and VI (*b*, *d*, and *f* plots) models. The grey, diagonal lines correspond to the 1:1 relation. Observed *versus* predicted models correspond to all the data (dotted lines) and to treatments where the intercept or the slope differed from 0 and 1, respectively (solid lines). Open circles represent the drought treatment in plant biomass plots and the fertilized treatment in C:N ratio plots. In the PV plots, senescent tiller treatments are represented as open circles for one tiller addition, open triangles for three-tiller addition, and crosses for no addition.

The coefficient of determination (R^2) of observed *versus* cross-validated predicted values was 0.13–0.24 higher for multiband than VI models, while both RMSD and RE were 10–40% lower for multiband than VI models (Table 2). Among plant properties, the proportion of photosynthetic vegetation showed a higher coefficient of determination and lower relative error than biomass or C:N. The general models lacked systematic error, as indicated by the high proportion of error accounted for by the unexplained variance (U_e) and by the lack of significant departure from 0 and 1 of the intercept and the slope. However, when these general models were evaluated only under the specific environmental conditions of each treatment, the goodness-of-fit decreased in all cases and a significant systematic error appeared in some cases: drought treatment for biomass estimations, fertilized treatment for C:N estimations based on vegetation indices, and most of the treatments with addition of senescent tillers when estimating the proportion of photosynthetic biomass for both VI and multiband approaches (Figure 1).

The spectral bands included in the general models were associated with absorption features related to specific biochemical components and differed among plant properties (Figure 2, Table 3). For biomass, the best multiband model was based on four bands: one in the red (682 nm), another in the near-infrared (932 nm), and two (1547 and 1797 nm) in the shortwave–infrared I region (1300–1900 nm, Figure 2(*a*)). The near-infrared band included in the model was highly correlated with its neighbouring bands (broad band), which indicates that other bands in the region were similarly useful, while the other three bands were correlated with a few neighbouring bands (narrow band), indicating a discrete absorption feature. These bands are related to photosystem II activity (682 nm) and structural carbohydrates such as cellulose (1547 nm) and hemicellulose (1797 nm). The best VI model combined a band in the visible (522 nm) with one in the red edge (712 nm, Figure 2(*b*)), related to low chlorophyll absorption and with nitrogen and protein content, respectively. This model was highly specific: few models (0.2% of possible models) combining one band in the red edge with another in the visible range reached values >90% of R^2 for the best model.

In regard to C:N ratio, the best general multiband model was based on five bands located in the red (677 nm), red edge (707 and 747 nm), and shortwave–infrared II (2187 and 2282 nm) regions (Figure 2(*c*)). The bands in 677 and 707 nm were narrow bands (neighbouring bands had much lower prediction ability), while those in 747, 2187, and 2282 nm were broader bands with similar prediction ability. These bands are related to the content of chlorophyll *a* and *b* (677 nm), nitrogen and protein (707 and 747 nm), cellulose (2187 and 2282 nm), and starch (2187 nm). The best VI model combined two bands in the shortwave–infrared I region (1542 and 1797 nm, Figure 2(*d*)), related to cellulose and starch, and hemicellulose content, respectively. This model was also very specific: only 0.1% of all the possible VI models reached >90% of R^2 for the best model.

In regard to the proportion of photosynthetic vegetation, the best general multiband model was based on seven bands distributed across the whole spectrum apart from the near-infrared region. There were four specific bands in the blue (467 nm), red (697 nm), red edge (722 nm), and shortwave–infrared I (1337 nm) regions and three broad bands in the shortwave–infrared I (1572 nm) and shortwave–infrared II (1967 and 2127 nm) regions (Figure 2(*e*)). These bands are related to contents of chlorophyll a, b, and carotenoids (467 nm), photosystem I activity (697 nm), nitrogen and protein content (722 nm), starch (1572 and 1967 nm), and lignin (2127 nm). The best VI model combined two bands in the shortwave–infrared I region, 1392 and 1797 nm (Figure 2(*f*)), related to the content of water and hemicellulose, respectively. This model was also quite specific: only a low proportion of other VI models (1.2% of possible models) reached >90% of R^2 for the best model. These VI models combined either one band in the red edge and another in the 1300–1700 nm region, or one band near 1400 nm and another in either the 1700 or 2200 nm region.

For those environmental conditions where general models presented significant systematic error (Figure 1), specific models based on either re-parameterization or new band selection satisfactorily accounted for the variation in plant properties (Table 4). Re-parameterization of the corresponding general models (i.e. same bands with different parameters) significantly reduced the relative error and the proportion of error accounted for by non-random components (non-random error) for all traits and treatments with the exception of biomass under drought, where only the systematic error was reduced. New band selection reduced the relative and the non-random error of re-parameterized models only for the multiband approach; new VI models reduced the relative but not the non-random error. Some of the newly selected bands for the multiband approach belonged to
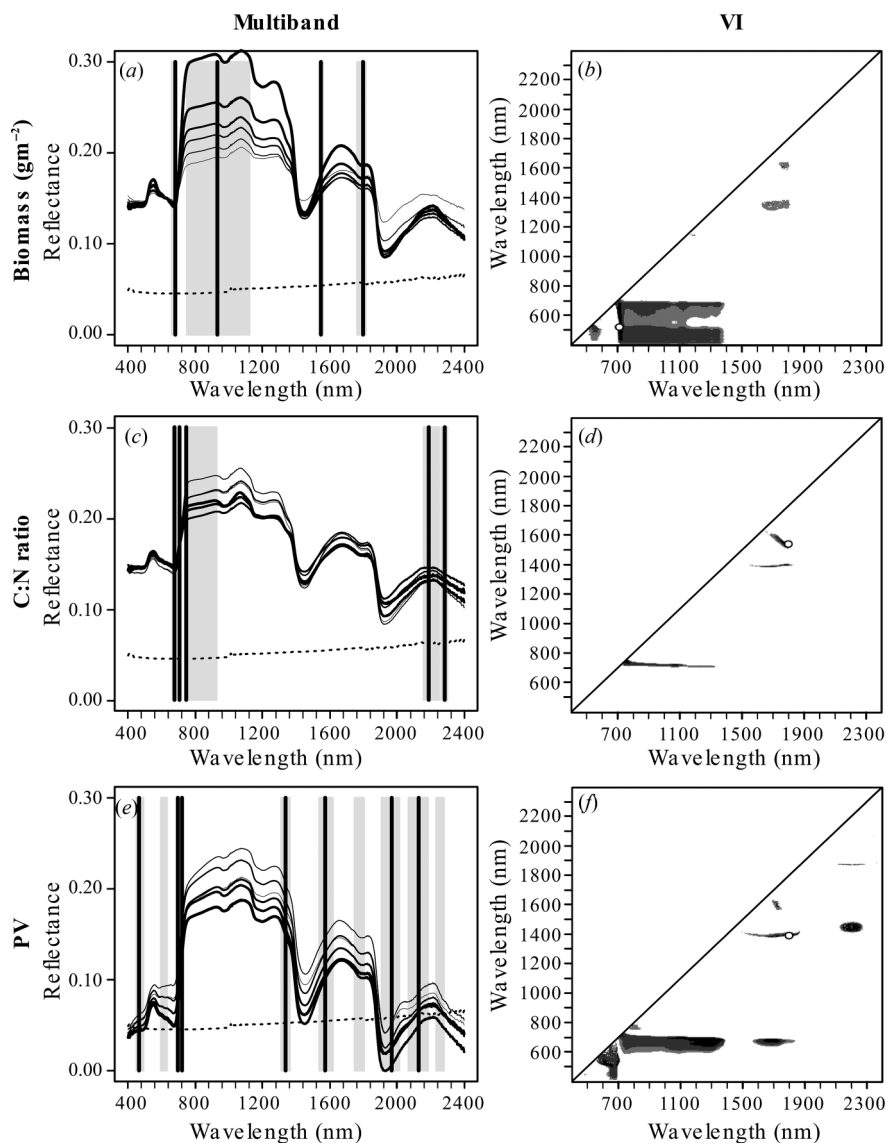
Figure 2. Selected bands for estimating plant biomass (B), C:N ratio, and the proportion of photosynthetic vegetation (PV) by multiband (*a*, *c*, and *e* plots) and VI (*b*, *d*, and *f* plots) models. Multiband plots show average reflectance of six increasing ranges of each plant property (thinner to thicker lines). The limits of the six ranges are: minimum, percentiles 5, 25, 50, 75, 95, and maximum. The black dotted line denotes the background reflectance without plants. Black vertical lines indicate bands selected for the optimal multiband models, and grey vertical lines indicate bands having a high correlation with selected bands ($R^2 > 0.99$). VI plots show wavebands used in the best VI models for each plant property. Open circles indicate the combination of bands with the highest R^2, while grey areas indicate those combinations of bands having $R^2 > 90\%$ (dark grey), $>80\%$ (grey), and $>70\%$ (light grey) of the maximum R^2. The R^2 values are the average of 1000 cross-validations (70% calibration, 30% evaluation).

Table 3. Wavelengths and spectral regions where known absorption features related to biochemical components occur (Curran 1989; Elvidge 1990), and selected bands in the present study by the two approaches (multiband and VI), for the three plant properties, and for general and treatment-specific models based on new bands. Biochemical components in bold letters indicate wavelengths of stronger absorption.

			Selected bands in the present study														
			Multiband							**VI**							
			Biomass		C:N ratio		Proportion of photosynthetic biomass			Biomass		C:N ratio		Proportion of photosynthetic biomass			
Wavelength (nm)	Spectral region	Biochemical components	General	Drought	General	General	General	1 tiller	3 tiller	Drought	General	General	Fertilized	General	0 tillers	1 tillers	3 tillers
400–500	Visible	Chlorophyll a, b, carotenoids					467										
530–600		Low chlorophyll absorption	522					597									532
640–670		Chlorophyll a, b			677								657				
680		Photosystem II	682										682				
700		Photosystem I					697										
700–800	Red edge	Nitrogen, protein			707, 747		722	707, 752			712						
930	Near infrared	Oil	932–	1062, 1337													
–	Shortwave infrared[1]	–			1337		1337		1362								1152
1390		Water, waxes												1392	1392		
1540		**Cellulose, starch**	1547						1547	139	1542						
1580		Starch					1572-									1607	
1720		Hemicellulose, pectins							1712								
1740		Arabinogalactan, rubisco		1752												1737	
1780		**Cellulose, sugar**								1777							
1790		Hemicellulose	1797						1912		1797	1797		1797	1797		

(Continued)

Table 3. (Continued).

Wavelengths and previously described related biochemical components			Selected bands in the present study														
			Multiband						VI								
			Biomass		C:N ratio	Proportion of photosynthetic biomass			Biomass		C:N ratio		Proportion of photosynthetic biomass				
Wavelength (nm)	Spectral region	Biochemical components	General	*Drought*	General	General	*1 tiller*	*3 tiller*	General	*Drought*	General	*Fertilized*	General	*0 tillers*	*1 tillers*	*3 tillers*	
1920	Shortwave infrared 2	Humic acid															
1960		Starch				1967											
2130		**Lignin,** protein				2127											
2180		**Nitrogen, protein,** Cellulose, Arabinogalactan			2187												
2280		Cellulose, starch			2282												
2350		Cellulose, protein, nitrogen		*2352*													

Note: Italic values were significant at $p < 0.05$.

Table 4. Performance of specific models fitted to the combination of treatments and plant properties for which the corresponding general model showed bias. Plant properties and treatments are: Bd = biomass under drought, C:Nf = C:N ratio under fertilization, and PV0, PV1, and PV3 are the proportion of photosynthetic biomass estimations with 0, 1, or 3 extra senescent tillers added. The table shows the relative error and non-random error (%) for the general model and specific models built by either the re-parameterization of the general model or the selection of new bands (shown in Table 3). Each value is the average of 1000 cross-validations that predicted 30% of the observations of each treatment on the basis of models generated from all other observations. The number of observations was 40 for Bd and C:Nf, and 48 for PV0, PV1, and PV3. Different letters indicate significant differences between models ($p < 0.05$). The non-random error is calculated as the sum of U_{bias} and U_e (see text for details).

Plant properties and treatments	Relative error			Non-random error (%)		
		Specific models			Specific models	
	General models	Re-parameterized	Based on new bands	General models	Re-parameterized	Based on new bands
Multiband						
Bd	0.28a	0.15b	0.11c	62a	22b	19c
PV1	0.07a	0.07b	0.05c	27a	21b	17c
PV3	0.12a	0.06b	0.05c	69a	22b	19c
VI						
Bd	0.20a	0.20a	0.14b	32a	19c	22b
C:Nf	0.49a	0.27b	0.11c	76a	39b	35c
PV0	0.06a	0.04b	0.04b	54a	16b	17b
PV1	0.08a	0.07b	0.05c	42a	17b	17b
PV3	0.15a	0.07b	0.06c	81a	20b	17b

the broad region of bands previously included in the general models (broad bands). For VI, the best combination of bands for the specific models coincided with those selected for the general models (or with combinations of bands reaching similar R^2 values) in only two of the five treatments where systematic error was observed (treatments with 0 and 1 extra senescent tillers added to estimate the proportion of photosynthetic biomass). The new bands included in these specific models were also related to known absorption features (Table 3). For the estimation of biomass under drought, the new bands were related to contents of protein (1752 and 2352 nm) and structural compounds (1392, 1777, and 2352 nm). For the estimation of C:N under fertilization, the new bands were related to photosynthesis (657 nm is related to chlorophyll content and 682 to photosystem II activity). For the estimation of the proportion of photosynthetic biomass under different levels of senescent biomass, the new bands were mainly spread along the visible (400–700 nm) and shortwave–infrared I (1300–1900 nm) regions.

4. Discussion

Simple general models based on reflectance of a few bands accounted for the variation in forage quantity and quality in single-species canopies under controlled background and illumination conditions. However, general models were inaccurate under certain environmental conditions. Biomass estimations were as accurate as in previous studies on pasture or grassland canopies under experimental conditions (Mutanga and Skidmore 2004), and more accurate than studies at the patch scale under field conditions (Chen et al. 2009; Clevers et al. 2007; Kawamura et al. 2008). C:N ratio estimations were less accurate than previous estimations performed on pastures at the landscape scale during the growing season and under contrasting grazing and fertilization conditions (Phillips, Beeri, and Liebig 2006). Our estimates of the proportion of photosynthetic vegetation were as accurate as those performed on grasslands and shrublands (Serrano et al. 2000). Our study differs from previous studies in regard to experimental variation of environmental conditions frequently acting on grasslands and pastures. Thus, it challenged the ability of remote sensing in estimating plant properties. The results showed that models performed satisfactorily in general, but failed under specific conditions such as drought (for plant biomass estimates), fertilization (for C:N ratio estimates), and different levels of senescent tillers (for estimates of the proportion of photosynthetic vegetation). For these situations, specific models achieved satisfactory accuracy levels. These results are in line with other studies showing that partitioning datasets into groups of homogeneous observations increases the accuracy of models for predicting forage quality (Mutanga, Skidmore, and Prins 2004; Serrano, Peñuelas, and Ustin 2002).

The difference in the selected bands between general and specific models was probably due to changes in canopy–light relationships associated with treatments. Consequently, different absorption features explained the variation in forage quantity and quality (Asner 1998; Curran 1989; Kokaly and Clark 1999). As previously seen for crops (Thenkabail, Smith, and De Pauw 2000), information on plant properties was based mainly on narrow or intermediate band widths (63% of the selected bands were <50 nm width). Besides, as expected, most of the selected bands (88%) coincided with known absorption properties. For predicting biomass quantity, the selected bands for the general model were located in the visible, red-edge, and near-infrared regions, where absorption features related with pigments occur (Ustin et al. 2009). By contrast, under the drought treatment, bands in the shortwave–infrared regions (SWIR I 1300–1900 and SWIR II 1900–2500 nm) became important for both VI and multiband models. This could be due

to the higher concentration of structural or dehydration avoidance compounds (i.e. cellulose, hemicellulose, lignin, and waxes) that appear under stress (Beard 1989) and that have absorption features at these regions. For predicting C:N ratio, the two bands in the general VI model were related to structural compounds (1542 and 1797 nm, Curran 1989; Elvidge 1990), while in the specific VI model for the fertilized treatment, bands were located in the flanks of red absorption (657 and 682 nm), which are correlated with chlorophyll (Ustin et al. 2009). For predicting the proportion of photosynthetic vegetation, the multiband model was based on a high number of bands distributed across the whole spectrum, which hinders interpretation, while both bands in the VI models were related to structural compounds. Specific models, based on different bands, were needed for each level of addition of senescent tillers, probably due to the strong variation in canopy conditions associated with the added extra non-photosynthetic material. At first glance, the need to change the predictors according to the conditions could be seen as a limitation of spectroscopy. Nevertheless, this reflects how it is possible to retrieve information on several plant properties provided that the influence of certain environmental conditions is considered.

Comparing both approaches, multiband models performed better than VI models for general, and similarly for specific, conditions. Similarly to Cho et al. (2007), general multiband models, based on a higher number of predictors (between 4 and 7 bands) presented better predictive power and fewer treatments with significant systematic error than models based on two-band vegetation indices. Besides, in agreement with previous studies (Clevers et al. 2007; Kawamura et al. 2008, 2010), a drastic reduction in the number of predictors (98–99%) did not diminish the predictive accuracy of multiband models compared with models based on the full spectrum. However, for specific models, predictive power was similar for both approaches. Re-parameterized models showed higher systematic error with the multiband approach than with the VI approach because of over-fitting of multiband models under more homogeneous canopy conditions. These results show that VI models, which are simpler and easier to interpret than multiband models, could be preferable for associating absorption features of specific wavebands with plant properties.

Our results have implications on the potential of remote sensing for estimating these plant properties under field conditions. The high proportion of narrow bands required for achieving the highest estimations indicates that hyperspectral sensors would be needed. Additionally, the inaccuracy of predictions of general models for some treatments indicates that it may be difficult to extrapolate models in space and time. Similar to the treatments evaluated here, variation in time and space due to biotic and abiotc factors affecting canopy reflectance can be a hindrance in the estimation of forage quantity and quality (Ollinger 2011). However, the more accurate predictions of biomass, C:N, or proportion of photosynthetic vegetation achieved when different bands were used for those treatments indicates that adaptive models changing bands for different conditions based on ancillary data could improve the predictive accuracy of general models. This kind of empirical study, performed under experimentally controlled environmental conditions and integrated with radiative transference models (i.e. PROSPECT, SAIL) and ecological theory can help to identify drivers of reflectance, facilitating upscaling from simple to complex canopies. It would then be possible to develop predictive models capable of dealing with the varying vegetation structure and background conditions occurring in natural multispecies canopies.

References

Asner, G. P. 1998. "Biophysical and Biochemical Sources of Variability in Canopy Reflectance." *Remote Sensing of Environment* 64: 234–253. doi:10.1016/S0034-4257(98)00014-5.

Beard, J. B. 1989. "Turfgrass Water Stress: Drought Resistance Components, Physiological Mechanisms, and Species-Genotype Diversity." In *Proceeding of 6th International Turfgrass Research Conference*, edited by H. Takatoh, Tokyo, July 31–August 5.

Beeri, O., R. Phillips, J. Hendrickson, A. B. Frank, and S. Kronberg. 2007. "Estimating Forage Quantity and Quality Using Aerial Hyperspectral Imagery for Northern Mixed-Grass Prairie." *Remote Sensing of Environment* 110: 216–225. doi:10.1016/j.rse.2007.02.027.

Bjørn-Helge, M., R. Wehrens, and K. H. Liland. 2011. *PLS: Partial Least Squares and Principal Component Regression*. R package version 2.3.0. http://CRAN.R-project.org/package=pls

Carrascal, L. M., I. Galván, and O. Gordo. 2009. "Partial Least Squares Regression as an Alternative to Current Regression Methods Used in Ecology." *Oikos* 118: 681–690. doi:10.1111/j.1600-0706.2008.16881.x.

Chen, J., S. Gu, M. Shen, Y. Tang, and B. Matsushita. 2009. "Estimating Aboveground Biomass of Grassland Having a High Canopy Cover: An Exploratory Analysis of in Situ Hyperspectral Data." *International Journal of Remote Sensing* 30: 6497–6517. doi:10.1080/01431160902882496

Cho, M. A., and A. K. Skidmore. 2009. "Hyperspectral Predictors for Monitoring Biomass Production in Mediterranean Mountain Grasslands: Majella National Park, Italy." *International Journal of Remote Sensing* 30: 499–515. doi:10.1080/01431160802392596.

Cho, M. A., A. K. Skidmore, and C. Atzberger. 2008. "Towards Red-Edge Positions Less Sensitive to Canopy Biophysical Parameters for Leaf Chlorophyll Estimation Using Properties Optique Spectrales Des Feuilles (PROSPECT) and Scattering by Arbitrarily Inclined Leaves (SAILH) Simulated Data." *International Journal of Remote Sensing* 29: 2241–2255. doi:10.1080/01431160701395328.

Cho, M. A., A. Skidmore, F. Corsi, S. E. van Wieren, and I. Sobhan. 2007. "Estimation of Green Grass/Herb Biomass from Airborne Hyperspectral Imagery Using Spectral Indices and Partial Least Squares Regression." *International Journal of Applied Earth Observation and Geoinformation* 9: 414–424. doi:10.1016/j.jag.2007.02.001.

Clevers, J. G. P. W., G. van der Heijden, S. Verzakov, and M. E. Schaepman. 2007. "Estimating Grassland Biomass Using SVM Band Shaving of Hyperspectral Data." *Photogrammetric Engineering and Remote Sensing* 73: 1141–1148. doi:10.14358/PERS.73.10.1141.

Curran, P. J. 1989. "Remote Sensing of Foliar Chemistry." *Remote Sensing of Environment* 30: 271–278. doi:10.1016/0034-4257(89)90069-2.

Darvishzadeh, R., A. Skidmore, M. Schlerf, C. Atzberger, F. Corsi, and M. Cho. 2008. "LAI and Chlorophyll Estimation for a Heterogeneous Grassland Using Hyperspectral Measurements." *ISPRS Journal of Photogrammetry and Remote Sensing* 63: 409–426. doi:10.1016/j.isprsjprs.2008.01.001.

Diaz-Solis, H., M. M. Kothmann, W. E. Grant, and R. De Luna-Villarreal. 2006. "Application of a Simple Ecological Sustainability Simulator (SESS) as a Management Tool in the Semi-Arid Rangelands of Northeastern Mexico." *Agricultural Systems* 88: 514–527. doi:10.1016/j.agsy.2005.07.008.

Elvidge, C. D. 1990. "Visible and Near Infrared Reflectance Characteristics of Dry Plant Materials." *International Journal of Remote Sensing* 11: 1775–1795. doi:10.1080/01431169008955129.

Filella, I., and J. Peñuelas. 1994. "The Red Edge Position and Shape as Indicators of Plant Chlorophyll Content, Biomass and Hydric Status." *International Journal of Remote Sensing* 15: 1459–1470. doi:10.1080/01431169408954177.

Freitas, S. R., M. C. S. Mello, and C. B. M. Cruz. 2005. "Relationships between Forest Structure and Vegetation Indices in Atlantic Rainforest." *Forest Ecology and Management* 218: 353–362. doi:10.1016/j.foreco.2005.08.036.

Gamon, J. A., C. B. Field, M. L. Goulden, K. L. Griffin, A. E. Hartley, G. Joel, J. Peñuelas, and R. Valentini. 1995. "Relationships between NDVI, Canopy Structure, and Photosynthesis, in Three Californian Vegetation Types." *Ecological Applications* 5: 28–41. doi:10.2307/1942049.

Grigera, G., M. Oesterheld, and F. Pacin. 2007. "Monitoring Forage Production for Farmers' Decision Making." *Agricultural Systems* 94: 637–648. doi:10.1016/j.agsy.2007.01.001.

Grime, J. P. 1977. "Evidence for the Existence of Three Primary Strategies in Plants and its Relevance to Ecological and Evolutionary Theory." *The American Naturalist* 111: 1169–1194. doi:10.1086/283244.

Hatfield, J. L., A. A. Gitelson, J. S. Schepers, and C. L. Walthall. 2008. "Application of Spectral Remote Sensing for Agronomic Decisions." *Agronomy Journal* 100: S-117–S-131. doi:10.2134/agronj2006.0370c.

Huston, J. E., and W. E. Pinchak. 1991. "Range Animal Nutrition." In *Grazing Management: An Ecological Perspective*, edited by R. K. Heitschmidt and J. W. Stuth, 12–24. Portland, OR: Timber Press.

Jackson, R. D., and A. R. Huete. 1991. "Interpreting Vegetation Indices." *Preventive Veterinary Medicine* 11: 185–200. doi:10.1016/S0167-5877(05)80004-2.

Jochims, F., C. H. E. C. Poli, P. C. F. Carvalho, D. B. David, N. M. F. Campos, L. Fonseca, and G. A. Amaral. 2013. "Grazing Methods and Herbage Allowances Effects on Animal Performances in Natural Grassland Grazed During Winter and Spring with Early Pregnant Ewes." *Livestock Science* 155: 364–372. doi:10.1016/j.livsci.2013.05.006.

Kawamura, K., N. Watanabe, S. Sakanoue, and Y. Inoue. 2008. "Estimating Forage Biomass and Quality in a Mixed Sown Pasture Based on Partial Least Squares Regression with Waveband Selection." *Grassland Science* 54: 131–145. doi:10.1111/j.1744-697X.2008.00116.x.

Kawamura, K., N. Watanabe, S. Sakanoue, H.-J. Lee, Y. Inoue, and S. Odagawa. 2010. "Testing Genetic Algorithm as a Tool to Select Relevant Wavebands From Field Hyperspectral Data for Estimating Pasture Mass and Quality in a Mixed Sown Pasture Using Partial Least Squares Regression." *Grassland Science* 56: 205–216. doi:10.1111/j.1744-697X.2010.00196.x.

Kokaly, R. F., and R. N. Clark. 1999. "Spectroscopic Determination of Leaf Biochemistry Using Band-Depth Analysis of Absorption Features and Stepwise Multiple Linear Regression." *Remote Sensing of Environment* 67: 267–287. doi:10.1016/S0034-4257(98)00084-4.

Mutanga, O., and A. K. Skidmore. 2004. "Narrow Band Vegetation Indices Overcome the Saturation Problem in Biomass Estimation." *International Journal of Remote Sensing* 25: 3999–4014. doi:10.1080/01431160310001654923.

Mutanga, O., A. Skidmore, and H. H. Prins. 2004. "Predicting in Situ Pasture Quality in the Kruger National Park, South Africa, Using Continuum-Removed Absorption Features." *Remote sensing of Environment* 89: 393–408. doi:10.1016/j.rse.2003.11.001.

Ollinger, S. V. 2011. "Sources of Variability in Canopy Reflectance and the Convergent Properties of Plants." *New Phytologist* 189: 375–394. doi:10.1111/j.1469-8137.2010.03536.x.

Peñuelas, J., J. A. Gamon, A. L. Fredeen, J. Merino, and C. B. Field. 1994. "Reflectance Indices Associated with Physiological Changes in Nitrogen- and Water-Limited Sunflower Leaves." *Remote Sensing of Environment* 48: 135–146. doi:10.1016/0034-4257(94)90136-8.

Phillips, R., O. Beeri, E. Scholljegerdes, D. Bjergaard, and J. Hendrickson. 2009. "Integration of Geospatial and Cattle Nutrition Information to Estimate Paddock Grazing Capacity in Northern US Prairie." *Agricultural Systems* 100: 72–79. doi:10.1016/j.agsy.2009.01.002.

Phillips, R. L., O. Beeri, and M. Liebig. 2006. "Landscape Estimation of Canopy C:N Ratios Under Variable Drought Stress in Northern Great Plains Rangelands." *Journal of Geophysical Research* 111: G02015. doi:10.1029/2005JG000135.

R Development Core Team. 2011. *R: A Language and Environment for Statistical Computing*. Vienna: R Foundation for Statistical Computing. ISBN 3-900051-07-0. http://www.R-project.org/

Reddy, G. S., C. L. N. Rao, L. Venkaratnam, and P. V. K. Rao. 2001. "Influence of Plant Pigments on Spectral Reflectance of Maize, Groundnut and Soybean Grown in Semi-Arid Environments." *International Journal of Remote Sensing* 22: 3373–3380. doi:10.1080/01431160152609218.

Roberts, D. A., S. L. Ustin, S. Ogunjemiyo, J. Greenberg, S. Z. Dobrowski, J. Chen, and T. M. Hinckley. 2004. "Spectral and Structural Measures of Northwest Forest Vegetation at Leaf to Landscape Scales." *Ecosystems* 7: 545–562. doi:10.1007/s10021-004-0144-5.

Schwarz, G. E. 1978. "Estimating the Dimension of a Model." *The Annals of Statistics* 6: 461–464. doi:10.1214/aos/1176344136.

Serrano, L., J. Peñuelas, and S. L. Ustin. 2002. "Remote Sensing of Nitrogen and Lignin in Mediterranean Vegetation from Aviris Data: Decomposing Biochemical from Structural Signals." *Remote Sensing of Environment* 81: 355–364. doi:10.1016/S0034-4257(02)00011-1.

Serrano, L., S. L. Ustin, D. A. Roberts, J. A. Gamon, and J. Peñuelas. 2000. "Deriving Water Content of Chaparral Vegetation from AVIRIS data." *Remote sensing of Environment* 74: 570–581. doi:10.1016/S0034-4257(00)00147-4.

Smith, E. P., and K. A. Rose. 1995. "Model Goodness-Of-Fit Analysis Using Regression and Related Techniques." *Ecological Modelling* 77: 49–64. doi:10.1016/0304-3800(93)E0074-D.

Soca, P., and R. Orcasberro. 1992. "Propuesta de Manejo del Rodeo de Cría en Base a Estado Corporal, Altura de Pasto y Aplicación de Destete Temporario." En: *Jornada Evaluación Física y Económica de Alternativas Tecnológicas Para La Cría En Predios Ganaderos*. EEMAC, Facultad de Agronomía, Paysandú.,Universidad de la República, Uruguay.

Thenkabail, P. S., R. B. Smith, and E. De Pauw. 2000. "Hyperspectral Vegetation Indices and their Relationships with Agricultural Crop Characteristics." *Remote Sensing of Environment* 71: 158–182. doi:10.1016/S0034-4257(99)00067-X.

Tucker, C. J. 1977. "Spectral Estimation of Grass Canopy Variables." *Remote Sensing of Environment* 6: 11–26. doi:10.1016/0034-4257(77)90016-5.

Ustin, S. L., A. A. Gitelson, S. Jacquemoud, M. Schaepman, G. P. Asner, J. A. Gamon, and P. Zarco-Tejada. 2009. "Retrieval of Foliar Information About Plant Pigment Systems from High Resolution Spectroscopy." *Remote Sensing of Environment* 113: SS67–SS77. doi:10.1016/j.rse.2008.10.019.

Wang, L., E. Hunt, J. Qu, X. Hao, C. S. Daughtry, and C. S. T. Daughtry. 2011. "Towards Estimation of Canopy Foliar Biomass with Spectral Reflectance Measurements." *Remote Sensing of Environment* 115: 836–840. doi:10.1016/j.rse.2010.11.011.